DESIGN ANALYSIS OF FERRITE SHEET ATTACHMENT FOR SAR REDUCTION IN HUMAN HEAD

M. T. Islam

Institute of Space Science (ANGKASA)
Universiti Kebangsaan Malaysia
UKM, Bangi Selangor 43600, Malaysia

M. R. I. Faruque

Department of Electrical, Electronic and Systems Engineering
Faculty of Engineering and Built Environment
Universiti Kebangsaan Malaysia
UKM, Bangi Selangor 43600, Malaysia

N. Misran

Department of Electrical, Electronic and Systems Engineering
Faculty of Engineering and Built Environment
Institute of Space Science (ANGKASA)
Universiti Kebangsaan Malaysia
UKM, Bangi Selangor 43600, Malaysia

Abstract—In this paper, reducing Specific Absorption Rate (SAR) with ferrite sheet attachment is investigated. The finite-difference time-domain method with Lossy-Drude model is adopted in this study. The methodology of SAR reduction is addressed and then the effects of attaching location, distance, size and material properties of ferrite sheet on the SAR reduction are investigated. Computational results show that the SAR averaging over 10 gm was better than that for 1 gm and SAR reduction of 57.75% is achieved for SAR 10 gm. These results show the way to choose a ferrite sheet with the maximum SAR reducing effect for phone model.

Corresponding author: M. T. Islam (tariqul@ukm.my).

1. INTRODUCTION

Cellular phone protection and the enforcement of pertinent exposure standards are issues in the current media, and regulatory agencies are motivated to assure that compliance testing is acceptable. IEEE Standard 1528 [1] and IEC 62209-1 specify protocols and process for the measurement of the peak spatial-average specific absorption rate (SAR) induced inside a simplified model of the head of the users of hand held radio transceivers (cellular phones). For example, the SAR limit specified in IEEE C95.1: 1999 is 1.6 W/kg in a SAR 1 gm averaging mass while that specified in IEEE C95.1: 2005 has been updated to 2 W/kg in a 10 gm averaging mass [2]. This new SAR limit specified in IEEE C95.1: 2005 is comparable to the limit specified in the International Commission on Non-Ionizing Radiation Protection (ICNIRP) guidelines [3].

The exposure limits are defined commonly in terms of the spatial peak SAR averaged either over any one gram or ten grams of tissue. Especially, the U.S. Federal Communication Commission (FCC) requires the routine SAR evaluation of phone model prior to device authorization or use since 1997. So there is a need to reduce an effort for reducing the spatial peak SAR in the design stage of phone model because the possibility of a spatial peak SAR exceeding the recommended exposure limit cannot be completely ruled out [2, 3]. The interaction of the cellular handset with the human head has been investigated by many published papers with considering; first, the effect of the human head on the handset antenna performance, including the feed-point impedance, gain, and efficiency [4–8], second, the impact of the antenna EM radiation on the user's head due to the absorbed power, which is measured by predicting the induced SAR in the head tissue [7–12].

The most used method to solve the electromagnetic problem dealt with this area is the finite-difference time-domain (FDTD) technique [10–13]. Although, in principle, the solution for general geometries does not require any additional effort with respect to the standard method, the technique requires the definition of the discretized space by assigning to each cell its own electromagnetic properties, which is not an easy process [12–15]. Specifically, the problems to be solved in SAR reduction need to correct representation of the cellular phone; anatomical representation of the head; alignment of the phone and the head and suitable design of ferrite sheet or other material.

Human exposure to electromagnetic (EM) radiation, as well as the pertinent health effects, constitutes a matter of raised public concern,

undergoing continuous scientific investigation. Various studies on this subject exist [8–20], most of which mainly delve into the consequences of mobile-phone usage. Yet, devices and communication terminals operating in other frequency bands have also gained substantial interest in the last 15 years. In [13], a ferrite sheet was adopted as protection attachment between the antenna and the human head. A reduction over 13% for the spatial peak SAR over 1 gm averaging was achieved. Study on the effects of attaching ferrite sheet for SAR reduction was presented [16, 21] and it was concluded that the position of shielding played an important role in the reduction effectiveness.

In [17, 22], for the SAR in human head, an effective approach is the use of a planar antenna integrated onto the back side (away from the head) of a phone model, but it brings additional design difficulties especially in achieving the required frequency bandwidth and radiation efficiency. Another approach is the use of a directional or reflecting antenna [13–16]. Such an antenna structure sacrifices the availability of signals received from all directions to the phone model. The mechanism of SAR reduction by ferrite sheet attachment was due to the suppression of surface currents on the front side of phone model [16]. However, the relationship between the maximum SAR reducing effect and the parameters such as attaching location, size and material properties of ferrite sheet remains unknown.

In [9, 16], a perfect electric conductor (PEC) reflector was placed between a human head and the driver of a folded loop antenna. The result showed that the radiation efficiency can be enhanced and the peak SAR value can be reduced. In [12], a study on the effects of attaching conductive materials to cellular phone for SAR reduction has been presented. It is shown that the position of the shielding material is an important factor for SAR reduction effectiveness. There is a necessity to make an effort for reducing the spatial peak SAR in the design stage of ferrite sheet because the possibility of a spatial peak SAR exceeding the recommended exposure limit cannot be completely ruled out. Two important parameters electric permittivity and magnetic permeability, determine the response of the materials to the electromagnetic propagation.

This paper is structured as follows. Section 2 describes the statistical analysis of the handset together with the SAM phantom head. FDTD method is used with positive meshing techniques for quick and correct analysis. Modeling and analyzing technique will be described in Section 3. Simulation and comparing results will be summarized in Section 4 and finally in Section 5 concluded the paper.

2. SIMULATION MODEL AND NUMERICAL TECHNIQUES

2.1. Model Description

The simulation model which includes the handset with helix type of antenna and the SAM phantom head provided by CST Microwave Studio (CST MWS) is shown in Fig. 1. Complete handset model composed of the circuit board, LCD display, keypad, battery and housing was used for simulation. The relative permittivity and conductivity of individual components were set to comply with industrial standards. In addition, definitions in [21–23] were adopted for material parameters involved in the SAM phantom head. In order to accurately characterize the performance over broad frequency range, dispersive models for all the dielectrics were adopted during the simulation [21]. Fig. 2 shows the dispersive permittivity of the

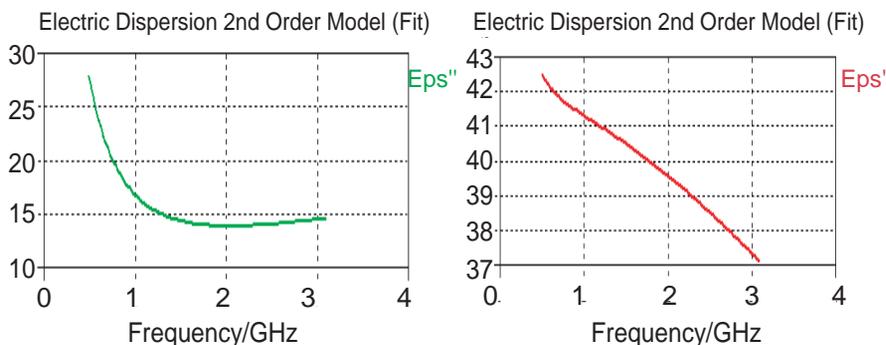**Figure 1.** Complete model used for simulation including handset and SAM phantom head.

Figure 2. Dispersive permittivity of the liquid in the SAM phantom head used for simulation.

Table 1. Electrical properties of materials used for simulation.

Phone Materials	ε_r	σ (S/m)
Circuit Board	4.4	0.05
Housing Plastic	2.5	0.005
LCD Display	3.0	0.02
Rubber	2.5	0.005
SAM Phantom Head		
Shell	3.7	0.0016
Liquid @ 900 MHz	40	1.42

liquid in SAM phantom head for simulation. The electrical properties of materials used for simulation are listed in Table 1. Helix type antenna constructed in a helical sense operating at 900 MHz for GSM application was used in the simulation model. In order to obtain high-quality geometry approximation for such helical structure, predictable meshing scheme used in FDTD method usually requires large number of hexahedrons which in turn makes it extremely challenging to get convergent results within reasonable simulation time.

2.2. Numerical Technique

CST MWS, based on the finite integral time-domain technique (FITD) proposed by Weiland in 1976 [23], was used as the main simulation instrument. In permutation of the perfect boundary approximation (PBA) and thin sheet technique (TST), significant development in geometry approximation with computation speed is achieved squashy highly accurate results. Non-uniform meshing scheme was adopted so that major computation endeavor was dedicated to regions along the inhomogeneous boundaries for fast and perfect analysis. Fig. 3 shows the mesh sight for two cut planes of the complete model indicating the area with denser meshing along the inhomogeneous boundaries. The minimum and maximum mesh sizes were 0.3 mm and 1.0 mm, respectively. A total of 2,097,152 mesh cells were generated for the complete model, and the simulation time was 1163 seconds (including mesh generation) for each run on an Intel Core^{TM} 2 Duo E8400 3.0 GHz CPU with 4 GB RAM system.

The analysis workflow in progress from the design of antenna with complete handset model in free space. The antenna was designed such that the S_{11} response was less than -10 dB over the frequency band of interest. SAM phantom head was then included for SAR calculation

using the standard definition as

$$SAR = \frac{\sigma}{2\rho}E^2$$

where E is the induced electric field (V/m); ρ is the density of the tissue (kg/m^3) and σ is the conductivity of the tissue (S/m). The resultant SAR values averaged over 1 gm and 10 gm of tissue in the head were denoted as SAR 1 gm and SAR 10 gm, respectively. These values were used as a benchmark to appraise the effectiveness in peak SAR reduction.
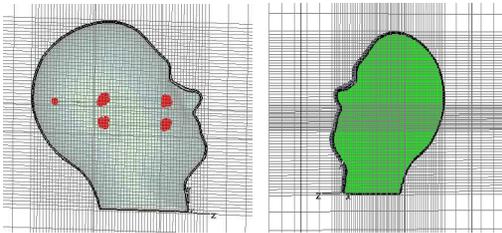

Figure 3. Mesh view for two cut planes of the complete model showing the nonuniform meshing scheme adopted for simulation.
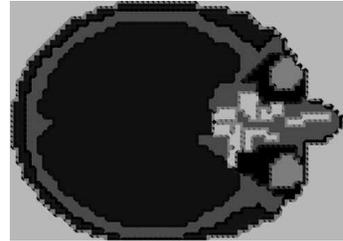

Figure 4. Human head model for FDTD computation.

Table 2. Dielectric tissue properties at 900 MHz and 1800 MHz [23, 24].

Material	Density, ρ (kg/m^3)	900 MHz		1800 MHz	
		Conductivity σ (S/m)	Relative Permittivity ε_r	Conductivity σ (S/m)	Relative Permittivity ε_r
Fat, Bone	1130	0.12	4.83	0.11	4.48
Muscle, Skin	1020	1.5	50.5	1.35	47.80
Brain	1050	1.11	41.7	1.09	39.50
Eyeball	1000	2.03	68.6	1.99	65.3

3. SAR REDUCTION BY FDTD METHOD WITH LOSSY DRUDE MODEL

3.1. Lossy-drude Model

The SAR reduction effectiveness and antenna performance with different positions, sizes and material properties of ferrite sheet will be analyzed. The head models used in this study was obtained from MRI-based head model through the whole brain Atlas website. Six types of tissues, i.e., bone, brain, muscle, eye ball, fat, and skin were involved in this model [22–26]. Table 2 shows their dielectric properties [23, 24]. Fig. 4 shows a horizontal cross-section through the eyes of this head model. The electrical properties of tissues were taken from [11]. Numerical simulation of SAR value was performed by FDTD method. The parameters for FDTD computation were as follows. In our Lossy-Drude simulation model, the domain were $128 \times 128 \times 128$ cells in FDTD method. The cell sizes were set as $\Delta x = \Delta y = \Delta z = 1.0$ mm. The computational domain was terminated with 8 cells PML. A helix antenna was modeled for this paper by thin-wire approximation. Simulations of ferrite sheet are performed by FDTD method with Lossy-Drude Model [23–26]. The method is utilized to understand the wave propagation characteristics of ferrite sheet.
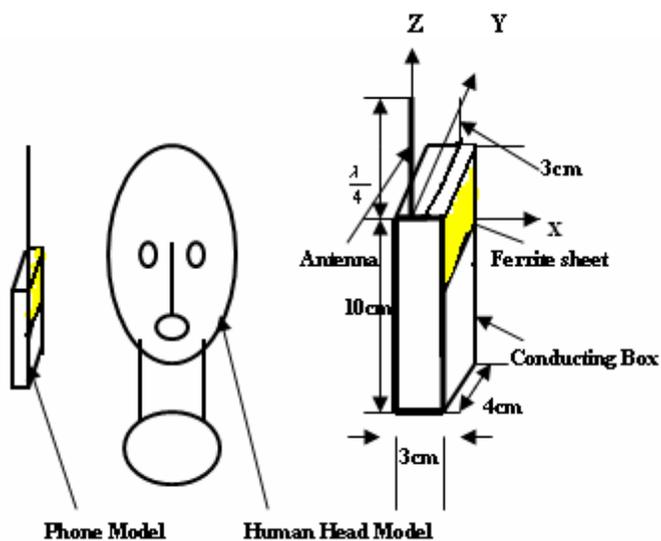

Figure 5. Models of head and portable telephone with attached ferrite sheet.

3.2. Analysis Method

Figure 5 shows a portable telephone model at 900 MHz for the present study. It was considered to be a quarter wavelength helix antenna mounted on a rectangular conducting box. The conducting box was 10 cm tall, 4 cm wide and 3 cm thick. The helix antenna was located at the top surface of conducting box. A ferrite sheet with a height of 90 mm, a width of 40 mm and a thickness of 3.5 mm was attached to the conducting box as shown in Fig. 5.

The head model was an anatomically based one constructed by our groups on the basis of an anatomical chart of a child adult head. It consists of about 2,097,152 cubical cells with a resolution of 1 mm. The FDTD method was employed in the numerical analysis. Its discretized formulations were derived from the following Maxwell's time-domain equations.

$$\frac{\delta H}{\delta t} = -\frac{1}{\mu_0 \mu_r'} \left(\nabla \times E \right) - \frac{\sigma^*}{\mu_0 \mu_r'} H \tag{1}$$

$$\frac{\delta E}{\delta t} = -\frac{1}{\varepsilon_0 \varepsilon_r'} \left(\nabla \times H \right) - \frac{\sigma^*}{\varepsilon_0 \varepsilon_r'} E \tag{2}$$

where $\sigma^* = \omega \mu_0 \mu_r''$ and $\sigma = \omega \varepsilon_0 \varepsilon_r''$. A space domain enclosing the human head and the phone model is shown in Fig. 5. The time step was set to $\frac{\delta}{\sqrt{3}c}$, where c is the speed of light, to guarantee the numerical stability. The time-stepping was performed for about eight sinusoidal cycles in order to reach a steady state. To absorb outgoing scattered waves, the second order Mur absorbing boundaries acting on electric fields were used. An antenna excitation was introduced by specifying a sinusoidal voltage across the one-cell gap between the helix and the top surface of the conducting box.

The antenna output power is defined as

$$P_{out} = P_{abs} + P_{ferr} + P_{rad}$$

$$= \frac{1}{2} \int_{Vh} \sigma \left| E \right|^2 dv + \frac{1}{2} \int_{Vf} \left(\sigma \left| E \right|^2 + \sigma^* \left| H \right|^2 \right) dv + \frac{1}{2} \text{Re} \left(\int_s E \times H^* \cdot \vec{n} \cdot ds \right) \tag{3}$$

where P_{abs} is the power absorbed in the head with a volume of V_h, P_{ferr} is the power dissipated in the ferrite sheet with a volume of V_f, and P_{rad} is the power radiated to the far-field, which can be calculated by integrating the normal component of the Pointing vector $E \times H^*$ over a surface S completely surrounding the head/phone model configuration.

4. IMPACT ON SAR OF FERRITE SHEET ATTACHMENT

In this section, ferrite sheet are placed between antenna and a human head then reducing the SAR value. In order to study SAR reduction of antenna operated at the GSM 900 band [27–29]. Different positions, sizes, and different materials of ferrite sheet for SAR reduction effectiveness are also analyzed by using the FDTD method in conjunction with a detailed human head model.

Figure 6 shows the simulation model which includes the handset with monopole type of helix antenna and the SAM phantom head that provided by CST MWS.

The dispersive models for all the dielectrics were adopted during the simulation in order to accurately characterize the ferrite sheet. The antenna was arranged in parallel to the head axis; the distance is varied from 5 mm to 20 mm; and finally 20 mm was chosen for comparison with ferrite sheet. Besides that, the output power of the mobile phone model need to be set before SAR is simulated. In this paper, the output power of the cellular phone is 500 mW at the operating frequency of
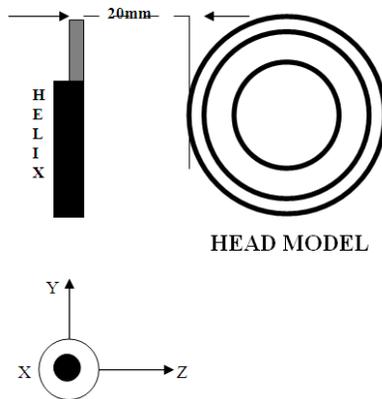

Figure 6. The head and antenna models for SAR calculation.

Table 3. Comparisons of peak SAR with ferrite sheet.

Tissue	SAR value (W/kg)
SAR value for [11]	1.28
SAR value for [19]	1.37
SAR value with ferrite sheet for 10 gm	0.676

0.9 GHz. In the real case, output power of the mobile phone will not exceed 250 mW for normal use, while the maximum output power can reach till 1 W or 2 W when the base station is far away from the mobile station (cellular phone). The SAR simulation is compared with the results in [11, 19] for validation, as shown in Table 3. The calculated peak SAR 1 gm value is 2.002 W/kg, and SAR 10 gm value is 1.293 W/kg when the phone model is placed 20 mm away from the human head model without ferrite sheet. This SAR value we achieved is better compared with the result reported in [23], which is 2.43 W/kg for SAR 1 gm. The ferrite sheet material is utilized in between the phone and head models, and it is found that the simulated value of SAR 1 gm and SAR 10 gm are 1.043 W/kg and 0.676 W/kg respectively. The reduction about 57.75% was observed in this study when a ferrite sheet is attached between phone and human head models for SAR 10 gm. This SAR reduction is better than the result reported in [15], which is 22% for SAR 10 gm. This is achieved due to the use of different radiating powers and impedance factors. Figs. 7–11 show the SAR value in the distance between phone and head models, width of ferrite sheet between 20–40 mm, thickness of ferrite sheet between 2–3.5 mm and height between 40–90 mm respectively.

The reduction efficiency of the SAR depends on its width and height. In order to definitely confirm this, 1 gm and 10 gm average SARs versus distance, width, thickness and height are plotted in the Figs. 7–11. In Fig. 7, it is shown that if the distance between phone
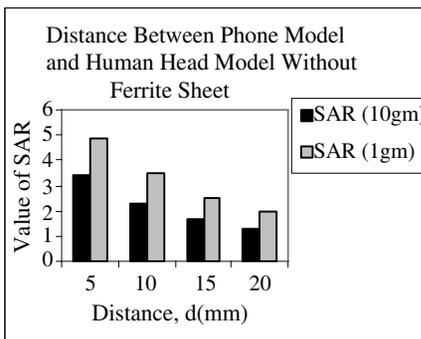

Figure 7. SAR value versus the distance between phone model and human head model without ferrite sheet.
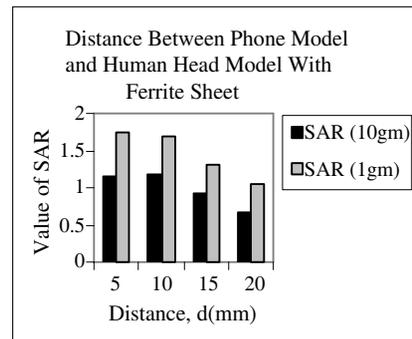
Figure 8. SAR value compared with the distance between phone model and human head model with ferrite sheet (Dimensions: Thickness 3 mm, Width 40 mm, and Height 80 mm).
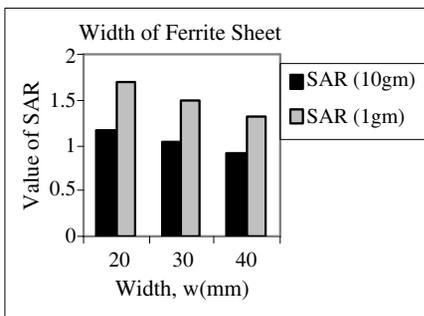
Figure 9. SAR value compared with the width of the ferrite sheet at a distance between the phone model to head model at 20 mm.
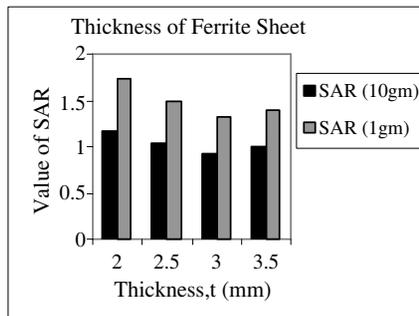
Figure 10. SAR value compared with the thickness of the ferrite sheet at a distance between the phone model to head model at 20 mm.
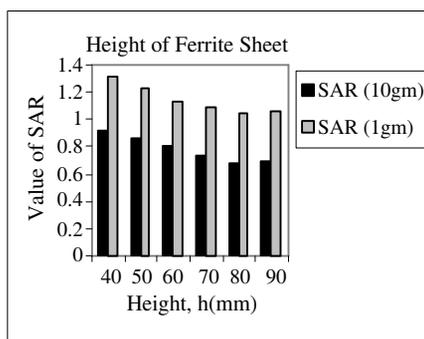

Figure 11. SAR value compared with the height of the ferrite sheet at a distance between the phone model to head model at 20 mm.

and human head models is varied then SAR value decreases. This is because dielectric constant, conductivity, density and magnetic tangent losses are also varied. Fig. 8 shows the SAR value with ferrite sheet attachment for 1 gm and 10 gm average SAR with the thickness 3 mm, width 40 mm, and height 80 mm. In Fig. 9, it can be observed that the SAR value reduces with the increase of the width of ferrite sheet at a distance between the phone model to head model at 20 mm. As shown in Fig. 10, the SAR value has decreased till the thickness of 3 mm, and different tendency, i.e., it started to increase after 3 mm at a distance between the phone model to head model at 20 mm. The height is varied till 90 mm at a distance between the phone model to head model at

20 mm in Fig. 11. From this figure, it can be illustrated that if the height of ferrite sheet increases SAR value also decreases up to height of 80 mm, and it started to increase after 80 mm. It can be observed that with ferrite sheet attachment the SAR value has been decreased for the case of 1 gm and 10 gm average SAR. The result imply that only suppressing the maximum current on the front side of conducting box contributes significantly to the reduction of spatial peak SAR. This is because the decreased quantity of the power absorbed in the head is considerably larger than that dissipated in the ferrite sheet.

5. CONCLUSIONS

The SAR reduction in human head by attaching ferrite sheet has been discussed in this paper. The average SAR value is with ferrite sheet is achieved about 0.676 for SAR 10 gm. Based on the 3-D FDTD method with lossy-Drude model, it is found that the peak SAR 10 gm of the head can be reduced by placing the ferrite sheet between the antenna and the human head.

ACKNOWLEDGMENT

REFERENCES

1. Recommended Practice for Determining the Peak Spatial-average Specific Absorption Rate (SAR) in the Human Head from Wireless Communications Devices: Measurement Techniques, IEEE Standard 1528-2003, 2003.

2. IEEE C95.1-2005, "IEEE standards for safety levels with respect to human exposure to radio frequency electromagnetic fields, 3 kHz to 300 GHz," Institute of Electrical and Electronics Engineers, New York, NY, 2005.

3. International Non-ionizing Radiation Committee of the International Radiation Protection Association, "Guidelines on limits on exposure to radio frequency electromagnetic fields in the frequency range from 100 kHz to 300 GHz," *Health Physics*, Vol. 54, No. 1, 115–123, 1988.

4. Christopoulou, M., S. Koulouridis, and K. S. Nikita, "Parametric study of power absorption patterns induced in adult and child head models by small helical antennas," *Progress In Electromagnetics Research*, PIER 94, 49–67, 2009.

5. Hirata, A., K. Shirai, and O. Fujiwara, "On averaging mass of SAR correlating with temperature elevation due to a dipole antenna," *Progress In Electromagnetics Research*, PIER 84, 221–237, 2008.

6. Mahmoud, K. R., M. El-Adawy, S. M. M. Ibrahem, R. Bansal, and S. H. Zainud-Deen, "Investigating the interaction between a human head and a smart handset for 4G mobile communication systems," *Progress In Electromagnetics Research C*, Vol. 2, 169–188, 2008.

7. Kouveliotis, N. K. and C. N. Capsalis, "Prediction of the SAR level induced in a dielectric sphere by a thin wire dipole antenna," *Progress In Electromagnetics Research*, PIER 80, 321–336, 2008.

8. Ebrahimi-Ganjeh, M. A. and A. R. Attari, "Interaction of dual band Helical and PIFA handset antennas with human head and hand," *Progress In Electromagnetics Research*, PIER 77, 225–242, 2007.

9. Kuo, L. C., Y. C. Kan, and H.-R. Chuang, "Analysis of a 900/1800-MHz dual-band gap loop antenna on a handset with proximate head and hand model," *Journal of Electromagnetic Waves and Applications*, Vol. 21, No. 1, 107–122, 2007.

10. Kouveliotis, N. K., S. C. Panagiotou, P. K. Varlamos, and C. N. Capsalis, "Theoretical approach of the interaction between a human head model and a mobile handset helical antenna using numerical methods," *Progress In Electromagnetics Research*, PIER 65, 309–327, 2006.

11. Fung, L. C., S. W. Leung, and K. H. Chan, "An investigation of the SAR reduction methods in mobile phone application," *2002 IEEE International Symposium on EMC*, Vol. 2, 656–660, Aug. 2002.

12. Habashy, T. M. and A. Abubakar, "A generalized material averaging formulation for modeling of the electromagnetic fields," *Journal of Electromagnetic Waves and Applications*, Vol. 21, No. 9, 1145–1159, 2007.

13. Ali, M. and S. Sanyal, "A numerical investigation of finite ground planes and reflector effects on monopole antenna factor using FDTD technique," *Journal of Electromagnetic Waves and Applications*, Vol. 21, No. 10, 1379–1392, 2007.

14. Okoniewski, M. and M. Stuchly, "A study of handset antenna and human body interaction," *IEEE Trans. Microwave Theory Tech.*,

Vol. 44, 1855–1864, Oct. 1996.

15. Wang, J. and O. Fujiwara, "Reduction of electromagnetic absorption in the human head for portable telephones by a ferrite sheet attachment," *IEICE Trans. Commune.*, Vol. E80-B, No. 12, 1810–1815, Dec. 1997.

16. Kiminami, K., A. Hirata, Y. Horii, and T. Shiozawa, "A study on human body modeling for the mobile terminal antenna design at 400 MHz band," *Journal of Electromagnetic Waves and Applications*, Vol. 19, 671–687, 2005.

17. Li, L. W., M. S. Leong, P. S. Kooi, and T. S. Yeo, "Specific absorption rates in human head due to handset antennas: A comparative study using FDTD method," *Journal of Electromagnetic Waves and Applications*, Vol. 14, 987–1000, 2000.

18. Chan, K. H., K. M. Chow, L. C. Fung, and S. W. Leung, "Effects of using conductive materials for SAR reduction in mobile phones," *Microwave and Optical Technology Letters*, Vol. 44, No. 2, 140–144, Jan. 2005.

19. Wang, J. and O. Fujiwara, "FDTD computation of temperature rise in the human head for portable telephones," *IEEE Trans. Microwave Theory Tech.*, Vol. 47, No. 8, 1528–1534, Aug. 1999.

20. Kuo, L. C., Y. C. Kan, and H. R. Chuang, "Analysis of a 900/1800 MHz dual-band gap loop antenna on a handset with proximate head and hand model," *Journal of Electromagnetic Waves and Applications*, Vol. 21, No. 1, 107–122, 2007.

21. Chou, H.-H., H. T. Hsu, H. T. Chou, K. H. Liu, and F. Y. Kuo, "Reduction of peak SAR in human head for handset applications with resistive sheets (R-cards)," *Progress In Electromagnetics Research*, PIER 94, 281–296, 2009.

22. Kuo, L. C., H. R. Chuang, Y. C. Kan, T. C. Huang, and C. H. Ko, "A study of planer printed dipole antennas for wireless communication applications," *Journal of Electromagnetic Waves and Applications*, Vol. 21, No. 5, 637–652, 2007.

23. Weiland, T., "A discretization method for the solution of Maxwell's equations for six-component fields," *Electronics and Communications (AEU)*, Vol. 31, 116, 1977.

24. Zygiridis, T. T. and T. D. Tsiboukis, "Assessment of human head exposure to wireless communication devices combined electromagnetic and thermal studies for diverse frequency bands," *Progress In Electromagnetics Research B*, Vol. 9, 83–96, 2008.

25. Elkaramany, E. M. A. and F. G. A. El-Hadeed, "Circuit models

for 2-dimensional EM absorption by biological bodies," *Progress In Electromagnetics Research*, PIER 66, 1–14, 2006.

26. Wu, B. I., F. C. A. I. Cox, and J. A. Kong, "Experimental methodology for non-thermal effects of electromagnetic radiation on biologics," *Journal of Electromagnetic Waves and Applications*, Vol. 21, No. 4, 533–548, 2007.

27. Hawang, J. N. and F.-C. Chen, "Reduction of the peak SAR in the human head with metamaterials," *IEEE Transactions on Antenna and Propagation*, Vol. 54, No. 12, 3763–3770, 2006.

28. Liu, Y., Z. Liang, and Z. Yang, "Computation of electromagnetic dosimetry for human body using parallel FDTD algorithm combined with interpolation technique," *Progress In Electromagnetics Research*, PIER 82, 95–107, 2008.

29. Ibrahiem, A., C. Dale, W. Tabbara, and J. Wiart, "Analysis of the temperature increase linked to the power induced by RF source," *Progress In Electromagnetics Research*, PIER 52, 23–46, 2005.